# Investigation of LS-DYNA® Modeling for Active Muscle Tissue

Sebastian Mendes, Dr. Chiara Silvestri, Prof. Dr. Malcolm H. Ray
*Department of Civil and Environmental Engineering*
*Worcester Polytechnic Institute*
*Worcester, MA, 01609, USA*

## Abstract

*This study is aimed at investigating and comparing one-dimensional and three-dimensional finite element models of active muscle tissue. Skeletal muscle is a very complicated biological structure to model due to its non-homogeneous and non-linear material properties as well as its complex geometry. Additionally, forces generated from muscle activation are directly related to the muscle length and contraction velocity. Finite element discrete Hill-based elements are largely used to simulate muscles in both passive and active states. There are, however, several shortfalls to utilizing one- dimensional elements, such as the impossibility to represent muscle physical mass and complex lines of action. Additionally, the use of one-dimensional elements restricts muscle insertion sites to a limited number of nodes causing unrealistic loading distributions. These limitations are partially solved with a three-dimensional solid muscle model, where discrete Hill-based elements are combined in series and parallel to solid elements possessing hypo-elastic material properties. Despite some instability, the model was concluded to be an improvement over purely one-dimensional muscle models.*

*Hill-type material models MAT_S15 and MAT_156 were considered for muscle discrete representation with use of spring and beam elements, respectively. Three-dimensional muscle tissue was then represented with superposition of beam (MAT_156) and shell elements (MAT_OGDEN_RUBBER). A finite element control model was developed with the goal of employing muscle models for a simplified replication of flexion and extension movements of the tibia bone. The primary objective of the control model was to compare properties and behaviors of spring, beam, and shell-beam muscle models. Two separate simulations were performed with each of the three control models to replicate the protagonist-antagonist muscle mechanism occurring with activation. For each simulation, data such as contraction velocity, muscle force and Von Mises stresses were obtained and compared.*

## Introduction

Previous efforts have been made to model skeletal muscle by utilizing one-dimensional finite elements. Olivetti (2006) investigated the role of muscle contraction as part of a research concerning finite element (FE) modeling of the human knee-thigh-hip (KTH). Specifically, an FE model of the lower extremities developed previously at the Lawrence Livermore National Laboratory (LLNL) was modified and used with the purpose of understanding injury mechanisms of the KTH during frontal car crashes. Discrete one-dimensional (1-D) Hill-based spring elements were used to model muscles. With this representation, the 1-D elements were unable to represent muscle mass and complex lines of action. Additionally, connections of the muscle tendon complex (MTC) to bone were restricted to a limited number of nodes causing unrealistic loading distributions. In reality, the MTC is connected to bone over large origin and insertion sites.

Chang et al. (2008) developed an FE model of the KTH including representation of muscles to investigate the effects of muscle forces on KTH injuries in frontal crashes. The model included 35 Hill-type muscles utilizing Material 156. Results indicated that active muscles have a definite effect upon the KTH fracture patterns during frontal collisions. The general lack of activation patterns in literature pertaining to the muscles of the lower extremity contributed to the limits of simulations.

A 3D solid muscle model was developed by Hedenstierna (2008) to investigate the effect of muscles in neck injury prevention. Discrete Hill-based elements were combined in series and parallel with solid elements possessing hypo-elastic material properties, in a combination called Super positioned Muscle Finite Element (SMFE). This 3D model aimed at capturing compressive stiffness, mass inertia, and contact interfaces between muscles for a more accurate muscle geometry and dynamic representation. Despite some instability, the SMFE model was concluded to be an improvement over purely 1-D muscle models.

In this research, an FE control model was developed to provide a conceptual replication of the flexion and extension of the knee joint (Spence, 1986; McGinnis, 2005). The flexion of the knee involves a group of muscles known as posterior thigh muscles (flexors), located behind the femur, which pull the tibia toward the femur about the knee joint. The extension of the knee involves a group of muscles known as anterior thigh muscles (extensors), located in front of the tibia, which pull the tibia away from the femur about the knee joint. The primary objective of the control model was to allow for a comparison between the properties and behaviors of the spring, truss, and shell muscle models

## Methodology

Two FE solid rectangular bars were modeled in LS-DYNA to represent the femur and tibia bones and connected at their mutual ends by a revolute joint (Figure 1). Each bar had a length of 45 cm, height of 3 cm, and width of 1.5 cm. These dimensions were chosen to broadly mimic the actual dimensions of average femur and tibia bones. The femur bone was constrained in all directions, while the tibia bone was allowed to rotate about the joint. The bars were modeled with elastic material with the same density of bone (1.90 g/cm$^3$) (Cameron et al., 1999).

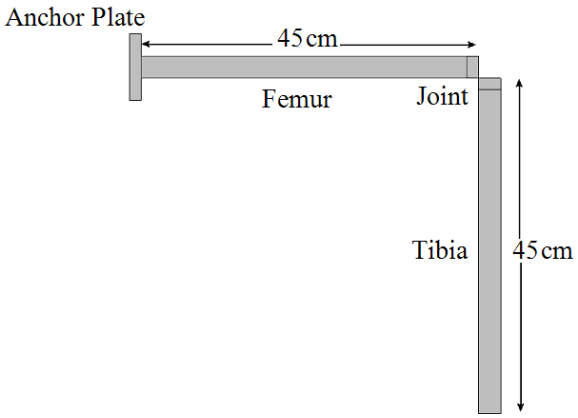


**Figure 1.** Profile view of control model.

The biceps femoris (BF) and the sartorius (S) muscles were chosen to represent the flexor and extensor muscles, respectively. Properties including mass, density, optimal muscle length, pennation angle, physiological cross section area (PCSA), maximum contraction velocity, and approximate peak isometric force were acquired for these muscles and are shown in Tables 1 and 2 (Lieber, 2002). Properties that were used for FE simulations to replicate these muscles with spring, truss and shell elements are included as well.

**Table 1.** Biceps femoris muscle property inputs (Lieber, 2002).

| Property | Biceps Femoris | BF - Spring | BF - Truss | BF - Shell |
|---|---|---|---|---|
| Mass (g) | 128 | - | - | 128 |
| Density (g/cm$^3$) | 1.056 | - | 1.056 | 1.056 |
| $L_o$ (cm) | 34.2 | 45 | - | - |
| Thickness (cm) | - | - | - | 0.35 |
| Pennation angle (˚) | 0 | - | - | - |
| PCSA (cm$^2$) | 12.8 | - | 0.256 | 0.256 |
| $V_{max}$ (cm/s) | 171 | 171 | - | - |
| Maximum strain rate (s$^{-1}$) | 5 | - | 5 | 5 |
| $F_{max}$ (N) | 320 | 320 | - | - |
| Peak isometric stress (N/cm$^2$) | 25 | - | 25 | 25 |

**Table 2.** Sartorius muscle property inputs (Lieber, 2002).

| Property | Sartorius | S - Spring | S - Truss | S - Shell |
|---|---|---|---|---|
| Mass (g) | 61.7 | - | - | 62 |
| Density (g/cm$^3$) | 1.056 | - | 1.056 | 1.056 |
| $L_o$ (cm) | 50.3 | 4.24 | - | - |
| Thickness (cm) | - | - | - | 0.65 |
| Pennation angle (˚) | 0 | - | - | - |
| PCSA (cm$^2$) | 1.7 | - | 0.034 | 0.034 |
| $V_{max}$ (cm/s) | 251.5 | 251.5 | - | - |
| Maximum strain rate (s$^{-1}$) | 5 | - | 5 | 5 |
| $F_{max}$ (N) | 42.5 | 42.5 | - | - |
| Peak isometric stress (N/cm$^2$) | 25 | - | 25 | 25 |

Two types of simulations were performed, considering different types of FE muscle representation (spring, truss and solid), for a total of six runs (Figure 2). The first type of simulation included only representation of the flexor muscle (biceps femoris), to allow for investigation of knee flexion by activation of the flexor muscle without the influence of the extensor muscle. The setup of the second type of simulation considered both the flexor muscle and the extensor muscle (sartorius), to allow for investigation of knee extension by activation of extensor muscle along with the influence of the passive flexor muscle. The activation of the flexor muscle was disabled while the activation of the extensor muscle was enabled for the second test setup. In all cases, identical linear activation curves were considered for muscle activation.

After a first attempt to use CONTACT_GUIDED_CABLE card to span the extensor muscle model from the femur to the tibia through the knee joint, it was decided to only consider direct lines of action between origin and insertion points. The extensor muscle was directly attached between nodes on the mutual ends of the femur and tibia mesh structures. This resulted, however, in shortening the length of the extensor muscle with respect to its actual length. Additionally, the actual locations of the origin and insertion points in bones could not be accurately replicated.

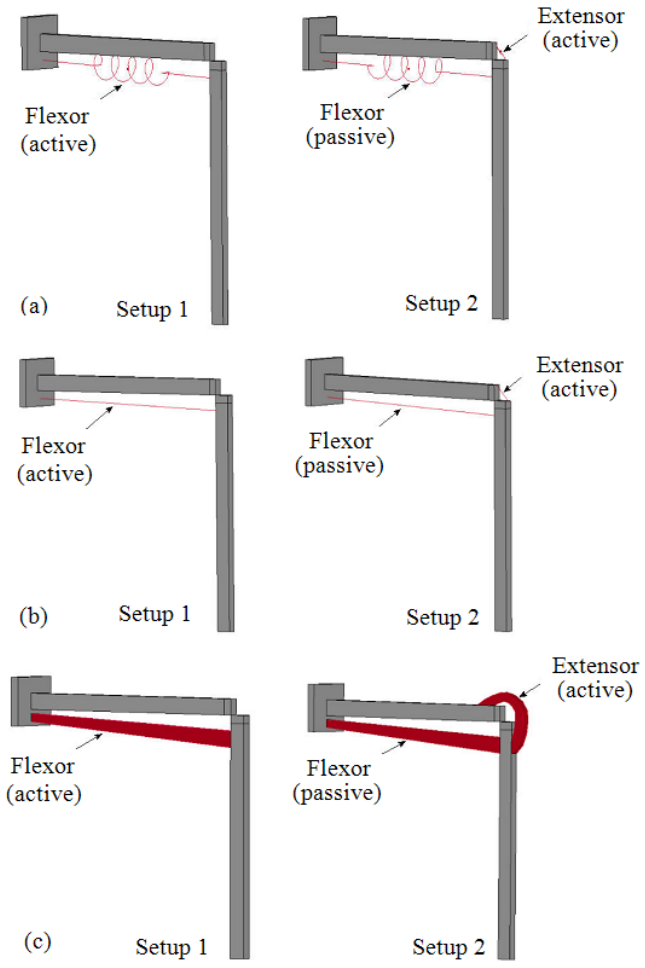


**Figure 2.** Configurations with (a) spring, (b) truss and (c) shell elements muscle model.

The flexor shell model consisted of a simple shell structure constructed of four interconnected shells giving the overall shell model a rectangular cross section. Four contractile truss elements were each attached to a corner node on each end of the shell so that each truss element's line of action was directed longitudinally along each of the four sides of the shell structure.

The structure of the extensor shell model was much more complex than the flexor shell model, having an indirect line of action around the knee joint. Interconnected shell elements were utilized to form a hollow tube with a rectangular cross section. The overall structure was then formed into the shape of a horseshoe when viewed from profile (Figure 3a). One end of the shell structure was connected to a set of nodes near the end of the femur (origin) while the other end was connected to the top of the tibia (insertion). Contractile truss elements were then integrated in series and parallel along the four edges of the shell structure (Figure 3b).

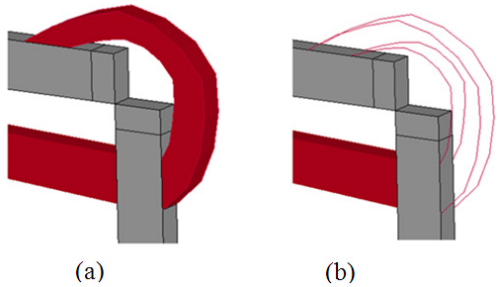


**Figure 3.** Extensor (a) shell and underlying (b) truss structures.

It was found from initial test runs that the use of Ogden rubber for shell models undergoing indirect lines of action failed to perform properly. Upon activation the contracting truss elements attempted to straighten out and in doing so caused the shells to tear apart. The use of elastic material, however, overcame this problem. Use of elastic material is acceptable since it was found previously that the dynamic behavior of Ogden rubber and elastic material is nearly identical in an SMFE combination (Chen et al., 1996). Therefore, elastic material with density of 1.056 g/cm$^3$, Poisson's ratio of 0.3 and Young's modulus of 1.0 MPa was used (Chen et al., 1996). As with the flexor shell model, each truss element was given a density of 1.056 g/cm$^3$.

The presence of contractile truss elements in the passive flexor shell muscle model produced unwanted preload forces in the muscle causing the SMFE combination to unexpectedly contract. Therefore, the contractile truss elements were removed from the passive flexor muscle in order to allow the active extensor muscle to extend the knee joint. In this way, the passive resistance of the flexor was provided solely by the Ogden rubber shell structure.

Initial runs of the extensor shell model showed that the passive resistance of the passive flexor prevented large extensions of the knee joint. This result was to be expected since the quadriceps muscles within the anterior compartment are the primary muscles which perform the extension of the knee, of which the sartorius plays a minor role. Additionally, the geometry of the extensor shell model itself was not realistic in terms of replicating the geometry of the sartorius which should have origin located on the pelvis rather than just above the knee joint. It was presumed that the addition of all the anterior compartment muscles would produce a realistic extension of the knee joint. The primary objective of the second control model, however, was only to compare properties and behaviors of spring, truss, and shell muscle models rather than producing an accurate and realistic simulation of the knee joint.

Figure 4 shows a schematic of the properties that are input into the SMFE combination.

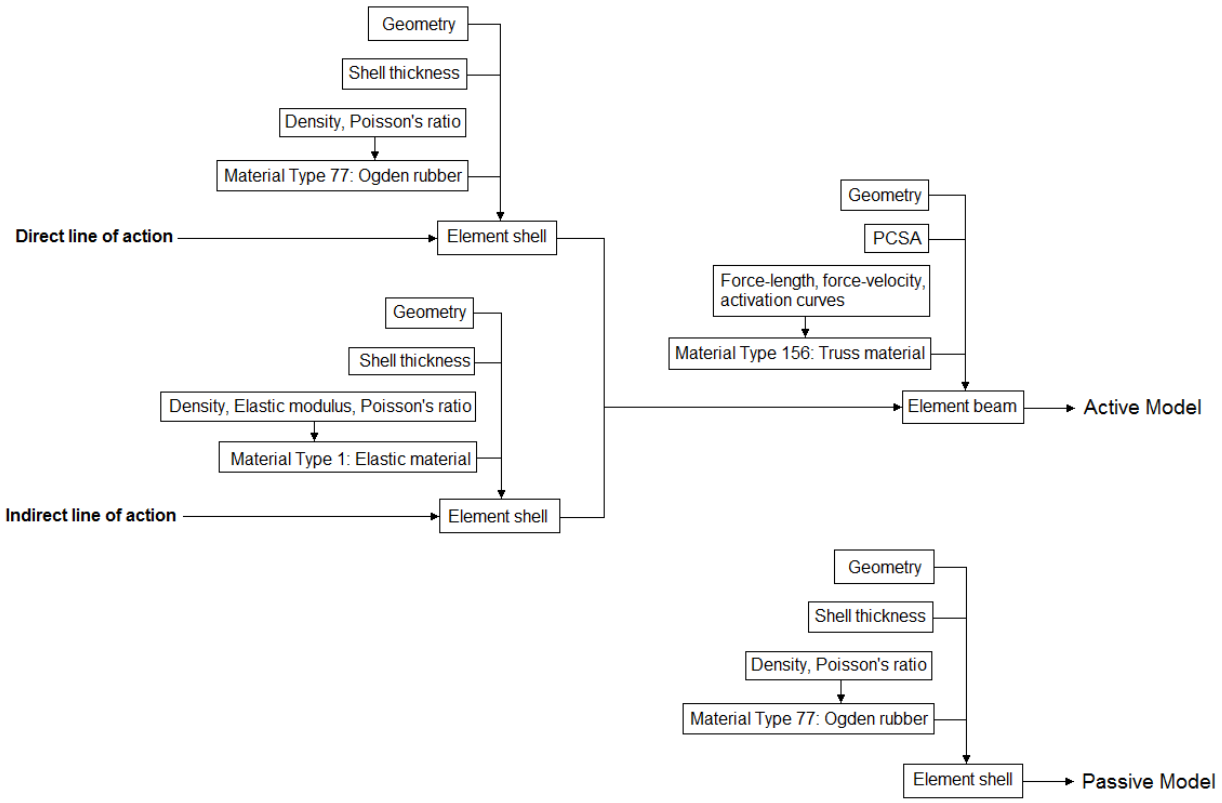


**Figure 4.** Schematic of property inputs for SMFE combination.

## Results and Discussion

**Sub-session: Knee Flexion**

Figure 5 demonstrates the flexion of the knee joint by the spring, truss and shell models in the first type of simulation (knee flexion).

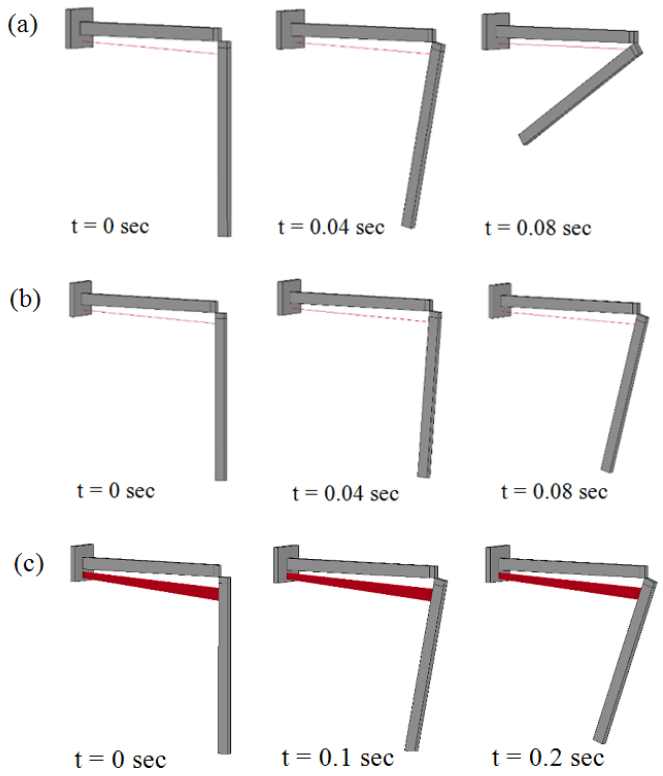


**Figure 5.** Flexion of knee joint with flexor (a) spring, (b) truss and (c) shell element models.

Figures 6 displays the resulting contraction velocities and forces for the spring and truss flexor muscle models obtained in simulations for knee flexion. Figure 7 displays the contraction velocity and muscle force for the shell flexor muscle model in this first simulation setup.

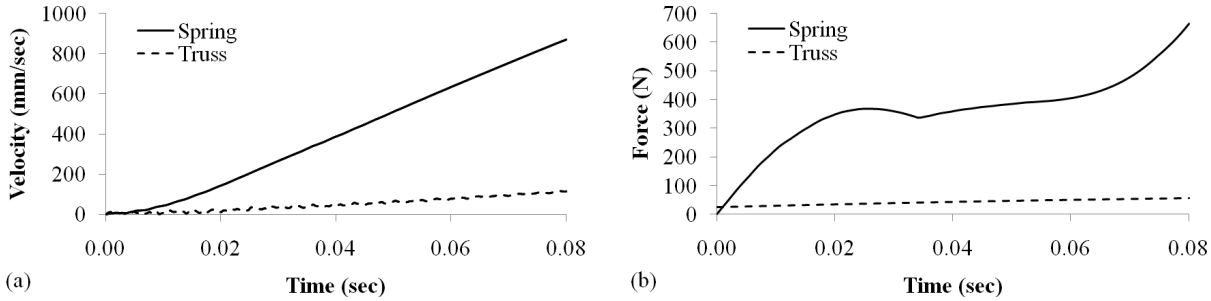


**Figure 6.** Contraction velocities (a) and muscle forces (b) of spring and truss flexor models.

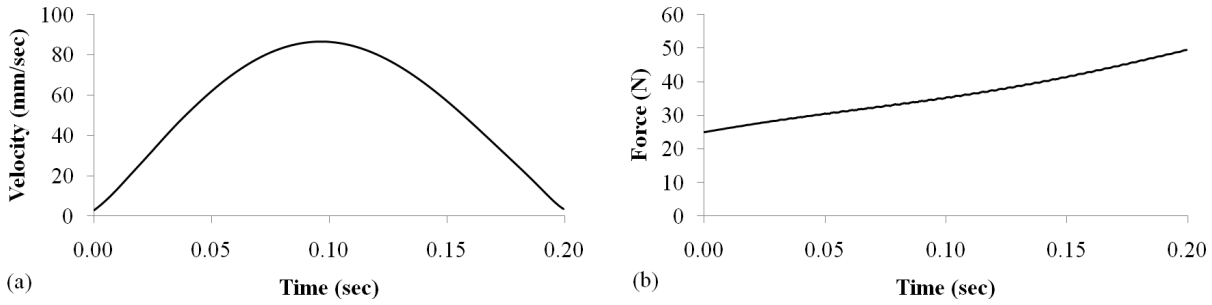


**Figure 7.** Contraction velocity (a) and muscle force (b) of shell flexor model.

The contraction velocity functions of the flexor spring and truss element models for the first simulation setup were similarly shaped albeit on different scales. The slightly unsteady contractile behavior exhibited by the truss model was presumed to be due to the rate of rotation allowed by the knee joint in LS-DYNA (CONSTRAINED_JOINT_REVOLUTE card) when coupled with a beam discrete element.

On the other side, the shape and scale of the muscle force of the flexor spring and truss element models for the knee flexion varied substantially. The contractile force of the spring model steadily rose and plateaued at 400 N before it rose to 625 N, while the contractile force of the truss model linearly rose from an initial value of 25 N up to 55 N The truss model exhibited much lower contractile velocities and induced much less contractile force than the spring model.

**Sub-session: Knee Extension**

Figure 8 demonstrates the flexion of the knee joint by the spring, truss and shell models in the first type of simulation (knee extension).

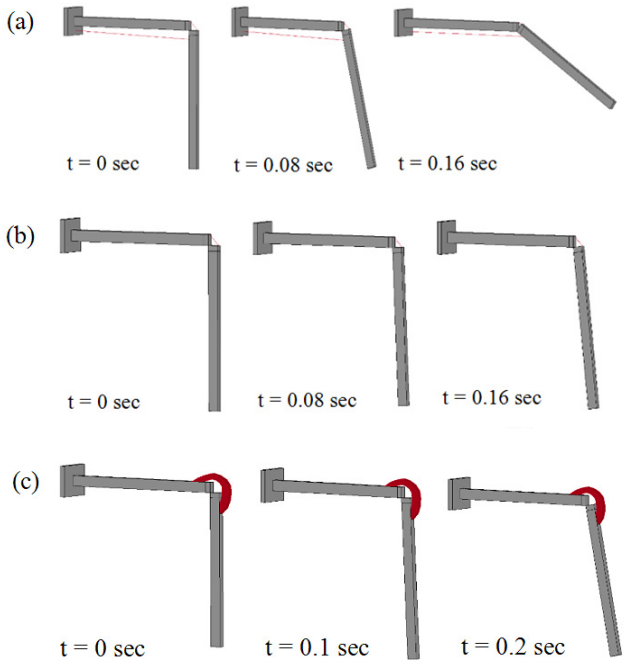


**Figure 8.** Extension of knee joint with extensor (a) spring, (b) truss and (c) shell element models.

Figure 9 displays the resulting contraction velocities and forces for the spring and truss extensor muscle models obtained in simulations from the knee extension simulations. Figure 10

displays muscle force for the shell extensor muscle model in the second simulation setup. It is noted that the contraction velocity of the shell extensor muscle model was excluded due to unstable data plots.

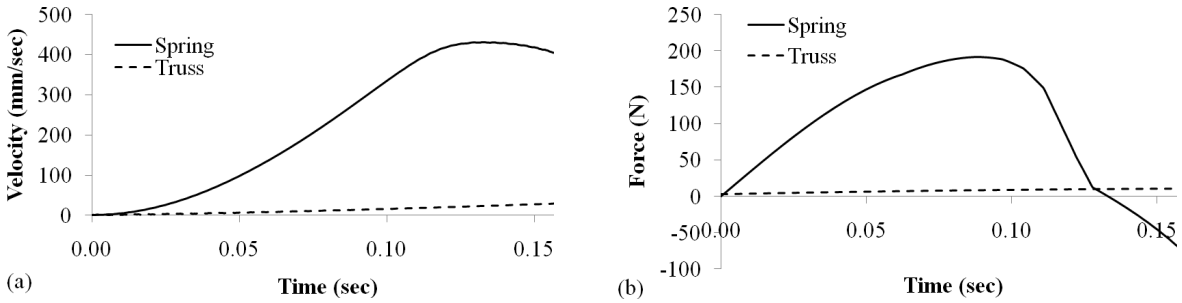


**Figure 9.** Contraction velocities (a) and muscle forces (b) of spring and truss extensor models.

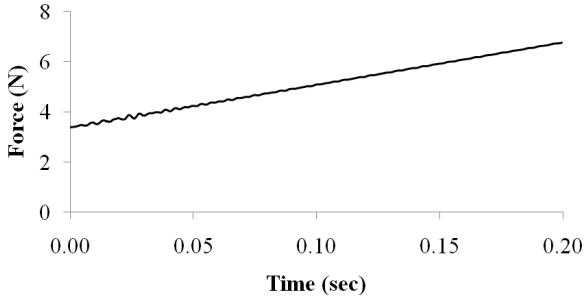


**Figure 10.** Muscle force of shell extensor model.

The contraction velocity of the extensor spring model steadily rose to approximately 0.43 m/s at 0.125 seconds. Additionally, the muscle force rose to a peak of 200 N before rapidly decreasing to zero. The lower overall velocity of the extensor spring model when compared to the flexor spring model is concluded to be partially due to the passive resistance effect of the passive flexor model and the lower overall force being induced by the extensor. As the active extensor muscle extended the knee joint, the passive flexor muscle resisted the extension.

It was discovered that the extension of the knee joint by the extensor truss model was impossible to perform due to the presence of the passive flexor truss model. The resistance of the passive flexor muscle overcame the contractile force of the active extensor muscle and thus caused the knee joint to undergo flexion instead of extension. This effect is concluded to be due to a preload force inherent to truss elements. When the flexor muscle was removed in order for the extensor muscle to perform the extension of the knee, the contraction velocity of the extensor muscle steadily rose to 0.025 m/s, while the muscle force steadily rose from an initial value of 3 N to 10 N. Again, the truss model exhibited much lower contractile velocities and forces than the spring model even without the passive resistance of the flexor muscle.

The contraction velocity function of the flexor shell model was similarly shaped to a concave down quadratic function with a peak velocity of approximately 0.08 m/s. The contractile force of the flexor shell model rose from an initial value of 25 N up to 50 N. Based on the comparable data, it can be seen that the contractile velocity and force of the shell model was approximately identical to the truss model but much lower than the spring model. It can be concluded, then, that the presence of the Ogden rubber shell material had very little influence on

the dynamic properties of the muscle. The primary role of the shells were to transmit and redistribute the stresses produced by the contractile elements throughout the muscle model and ultimately to the origin and insertion points. Additionally, the shells allowed for indirect lines of action by "guiding" the contractile action of the truss elements about joints.

The stress distributions on the isotropic elastic bars are presumably unrealistic since real bone possesses orthotropic material properties. The FE analyses demonstrate the varying stress distributions produced by each muscle model. Figure 11 shows Von Mises stress distribution on flexor insertion region for each muscle model at the approximate midpoint of flexion. Figure 12 shows the stress distribution on the extensor insertion region at the approximate midpoint of extension.

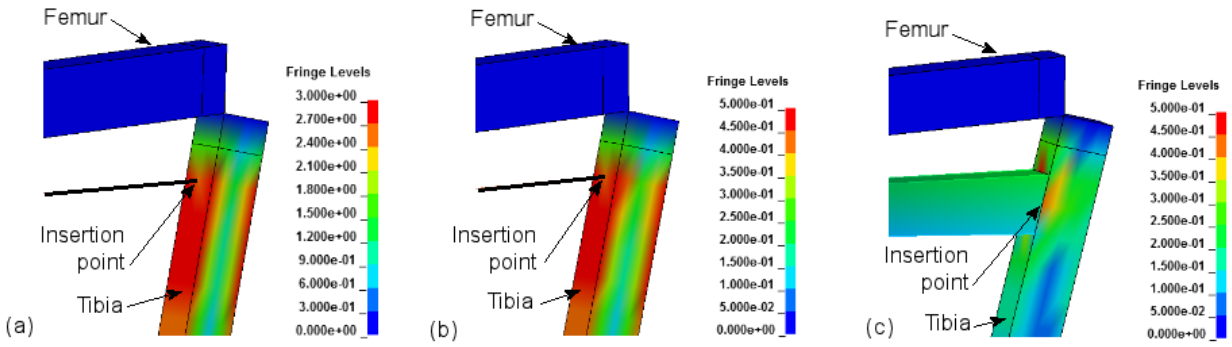


**Figure 11.** Von Mises stress distribution (N/mm$^2$) at insertion sites for (a) spring, (b) truss and (c) shell flexor model.

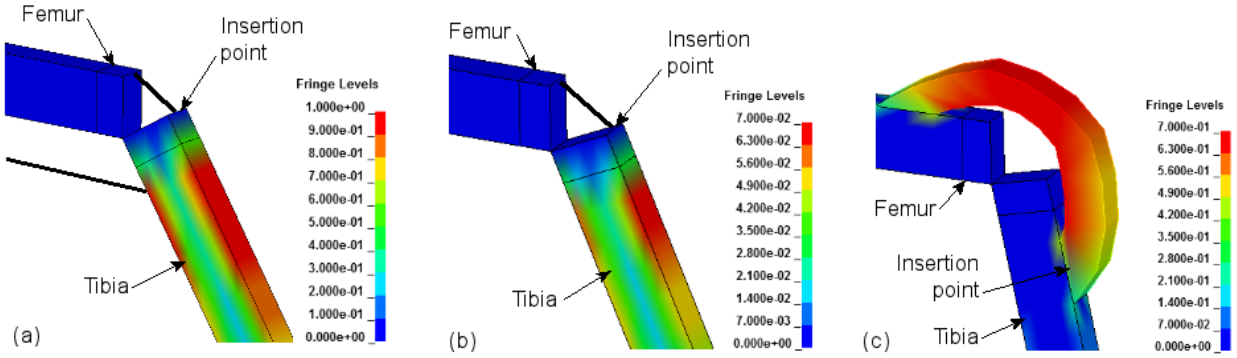


**Figure 12.** Von Mises stress distribution (N/mm$^2$) at insertion sites for (a) spring, (b) truss and (c) shell extensor model.

Stress distribution caused by each muscle model varied considerably. The spring and truss models produced peak stress areas concentrated primarily below the actual insertion point for both flexion and extension actions. This concentration of stress was most likely due to the contraction of the muscle producing bending stresses within the tibia. The red areas were indicative of the extreme fibers of the tibia undergoing stress from the flexure. The shell model produced smaller magnitudes of stress over a less concentrated area. As expected, the stress gradually decreased as the distance from the insertion point gradually increased.

## Conclusions

In conclusion, this work showed that the most realistic muscle model seems to be the SMFE combination, with use of shell elements and inclusion of contractile truss elements. For active muscles having direct lines of action, Ogden rubber should be utilized as the shell material with truss elements in parallel. Active muscles having indirect lines of action should utilize elastic material with truss elements in parallel and series. For passive muscles, the truss elements should be removed leaving only the shell structure.

The spring, truss, and shell element models seem to have similar levels of flexibility in terms of adjusting physical and dynamic properties in order to conform to different muscles. However, the SMFE combination has several advantages over the spring and truss models. First, the SMFE combination is able to simulate muscle mass by adjusting the shell density and thickness. Second, indirect lines of action are able to be produced. Finally, realistic stress distributions on the origin and insertion points on bone may be reproduced. Specifically, the force produced by the muscle is inherently distributed due to the presence of several truss elements, and is further distributed by the presence of shell elements which served to partially transmit the force from the truss elements to bone.

Despite the advantages of the SMFE combination over one-dimensional elements, there still remain many shortfalls. The fundamental combination of shell elements and contractile truss elements seems to be relatively unstable for long periods of activation. Additionally, the response of truss elements to corresponding activation levels is rather sluggish causing an SMFE model's response to nonlinear activation curves to be unpredictable. Furthermore, the use of shell elements means that the mass of the muscle is distributed unrealistically to the surface of the muscle.

The abandonment of a combination of two types of elements, i.e. truss and shell elements, could be replaced by a single type of element and corresponding material that performs the functions of both. The exploration of thermal materials which expand or contract based on temperature inputs is a plausible direction for future work. Varying inputs of temperature data could be coupled to specific dynamic properties of muscle obtained from literature and made to control the behavior of the muscle. When joined with solid elements, thermal material may be able to accurately replicate the physical and dynamic properties of muscle to an unprecedented level.

## Acknowledgments

This project has been sponsored by the National Transportation Biomechanics Research Center of the National Highway Traffic Safety Administration (NHTSA) under contract DTNH22-04-H-01424, Analytical Crash Simulation.

## References

Cameron, John R., Skofronick, James G., and Grant, Roderick M. (1999). *Physics of the Body*, 2nd Edition. Madison, WI: Medical Physics Publishing.

Chang, C.Y., Rupp, J.D., Kikuchi, N., Schneider, L.W. (2008). "Development of a finite element model to study the effects of muscle forces on knee-thigh-hip injuries in frontal crashes." *Stapp Car Crash Journal*., 1, 475-504.

Chen, Eric J., Novakofski, J., Jenkins, W.K., and O'Brien, W.D. (1996). "Young's modulus measurements of soft tissues with application to elasticity imaging." *IEEE Transactions On Ultrasonics, Ferroelectrics, and Frequency Control.*, 43(1), 191-194.

Hedenstierna, S. (2008). "3D finite element modeling of cervical musculature and its effect on neck injury prevention." Doctoral thesis, Royal Institute of Technology, Stockholm, Sweden.

Lieber, R.L. (2002). *Skeletal Muscle Structure, Function, & Plasticity: The Physiological Basis of Rehabilitation*, 2nd Edition. Baltimore, MD: Lippincott Williams & Wilkins.

McGinnis, P.M. (2005). *Biomechanics of Sport and Exercise*, 2nd Edition. Champaign, IL: Human Kinetics.

Olivetti, N., (2006). “Development of a Hill’s model of the human knee-thigh-hip region for frontal car crash simulations.” Thesis, Politecnico di Milano, Milan, Italy.

Spence, A.P. (1986). *Basic Human Anatomy*, 2nd Edition. Menlo Park, CA: The Benjamin/Cummings Publishing Company, Inc.